Sevastyanov G.M. Plane-Strain Extrusion of a Green Type Porous Plastic Material through a Wedge-Shaped Die // Вестник Пермского национального исследовательского политехнического университета. Механика. – 2022. – № 2. – С. 5–9. DOI: 10.15593/perm.mech/2022.2.01

Sevastyanov G.M. Plane-Strain Extrusion of a Green Type Porous Plastic Material through a Wedge-Shaped Die. *PNRPU Mechanics Bulletin*, 2022, no. 2, pp. 5-9. DOI: 10.15593/perm.mech/2022.2.01

пермский политех

ВЕСТНИК ПНИПУ. МЕХАНИКА
№ 2, 2022
PNRPU MECHANICS BULLETIN
https://ered.pstu.ru/index.php/mechanics/index

Research article

DOI: 10.15593/perm.mech/2022.2.01
UDK 539.374

PLANE-STRAIN EXTRUSION OF A GREEN TYPE POROUS PLASTIC MATERIAL THROUGH A WEDGE-SHAPED DIE

G.M. Sevastyanov

Institute of Machinery and Metallurgy, Khabarovsk Federal Research Center FEBRAS, Komsomolsk-on-Amur, Russian Federation

ARTICLE INFO

Received: 03 February 2022
Approved: 23 June 2022
Accepted for publication: 08 July 2022

Keywords:
porous solids, plasticity, Green type yield condition, Gurson criterion, plane-strain condition, wedge-shaped die.

ABSTRACT

This paper presents the solutions for the plane-strain extrusion of porous material. We consider the problem of a stationary plastic flow through a wedge shaped die. We neglect friction between the die and the deformed material since it is rather a negative effect and should be avoided in manufacturing. The elliptic Green type yield condition and its piecewise-linear approximation are adopted for this problem. In the last case, we obtain analytical solution that links extrusion pressure and area reduction to the initial and final density of the porous material. For elliptic Green yield condition the problem reduced to nonlinear ODE that integrated numerically. The results are compared with known solution for Gurson model. The extrusion pressure predicted by the piecewise-linear model is lower than what obtained by the elliptic Green model. In turn, the pressure predicted by elliptic Green model is lower than the pressure obtained in the frame of Gurson model. At low values of area reduction, all three models predict approximately the same extrusion pressure. With a small initial porosity of the material, the Gurson model gives results that are close to the elliptic Green model, and with a large initial porosity, to the piecewise-linear Green model.

Extrusion is a valuable technological process that has long been used for continuous metal processing as well as in pharmacy and food industry [1–3].

When the die walls are smooth enough and the taper angle is small, a radial flow of the material is realized during extrusion. Plane strain radial plastic flow is one of the classical problems in the theory of plasticity. The first known solution was obtained by Nadai [4], who determined the stress field in an ideal plastic material. The stationary velocity field corresponding to this solution was found by Hill [5] and, independently, by Sokolovsky [6]. Sokolovsky also found a complete solution to the problem for the material with power-law hardening according to the Hollomon equation. The result of Durban and Budiansky [7] is obtained for linear-hardening material (Ludwik equation). Haddow and Danyluk obtained an elastic-plastic solution of the same problem for non-hardening material in the framework of the Prandtl – Reuss theory [8]. Some other analytical and numerical results can be found in [9–12]. All the mentioned results were obtained for plastically incom-

© **Georgiy M. Sevastyanov** – CSc of Physical and Mathematical Sciences, Senior Researcher,
e-mail: akela.86@mail.ru, iD: 0000-0003-4755-5305

pressible materials. Plastically compressible (porous) materials can be described by the classical Mohr – Coulomb, Drucker – Prager, or Mises – Schleicher yield conditions. Although the associated plasticity for these yield conditions can leads to known discrepancies between the calculated volumetric strain and the experimental one, they often used to construct the models of complex media on the base of micromechanical solutions [13–15]. More precise yield conditions (for example, Green type models [16] and Gurson model [17]) are explicitly depend on the relative density (or porosity) of the material. For the Gurson model, an approximate analytical solution (of the first order in porosity) for stationary plane-strain radial plastic flow is known [18]. The Gurson model is also utilized to analyze plane-strain extrusion in [19–21]. Numerical results for the anisotropic model are presented in [22]. For Green type models, a number of results for axisymmetric extrusion were presented [23–25]; also the analytical solution [26; 27] for equal channel angular extrusion can be mentioned.

The present paper provides the solutions to the plane-strain problem of a stationary plastic flow through a wedge shaped die (Fig. 1). For the piecewise-linear Green type criterion, an exact analytical solution is obtained. For elliptic Green yield condition the problem reduced to nonlinear ODE that integrated numerically. As in [18; 28], friction between the die and the deformed material is neglected since it is rather a negative effect and should be avoided in manufacturing. The results are compared with solution [18] for Gurson model.

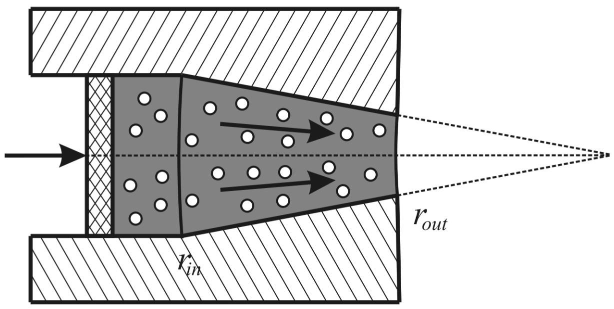

Fig. 1. Plane-strain extrusion through a wedge-shaped die

1. Plane-strain radial flow

The problem with cylindrical symmetry is considered. The radial flow is described by velocity vector $\mathbf{v} = v_r \mathbf{e}_r$, $v_r < 0$. It is assumed that the cylindrical surface $r = r_0$ is a free boundary (see Fig. 1).

The strain rate tensor has the following form

$$\mathbf{D} = \frac{1}{2}\left[\left(\nabla \otimes \mathbf{v}\right)^T + \left(\nabla \otimes \mathbf{v}\right)\right] = \\ = \frac{\partial v_r}{\partial r}\mathbf{e}_r \otimes \mathbf{e}_r + \frac{v_r}{r}\mathbf{e}_\varphi \otimes \mathbf{e}_\varphi .$$

For stationary flow, the continuity equation

$$\nabla \cdot \left(\rho \mathbf{v}\right) = -\partial\rho/\partial t = 0.$$

is satisfied, where t is the time, ρ is the dimensionless density of the porous material (the value $\rho = 1$ corresponds to a porosity-free material), $\nabla = \mathbf{e}_r \frac{\partial}{\partial r} + \mathbf{e}_\varphi \frac{1}{r}\frac{\partial}{\partial \varphi} + \mathbf{e}_z \frac{\partial}{\partial z}$ is the Hamiltonian. Hence, for the problem under consideration, it follows that

$$r\rho v_r = \text{const}. \quad (1)$$

From (1) it follows that

$$L = \frac{D_{rr}}{D_{\varphi\varphi}} = -\left(1 + \frac{r}{\rho}\frac{d\rho}{dr}\right). \quad (2)$$

The equilibrium equation $r\left(\partial\sigma_{rr}/\partial r\right) + \sigma_{rr} - \sigma_{\varphi\varphi} = 0$ with respect to (2) takes the form

$$\rho\frac{\partial\sigma_{rr}}{\partial\rho} = \frac{\sigma_{rr} - \sigma_{\varphi\varphi}}{L+1}. \quad (3)$$

From (2) it also follows that density distribution obeys the equation

$$\ln\frac{r_{out}}{r} = -\int_{\rho}^{\rho_{out}} \frac{1}{L(p)+1}\frac{dp}{p}. \quad (4)$$

2. Green type elliptic yield criterion

We utilize the elliptic Green yield condition and the associated flow rule

$$\Phi = \left(\sigma/\sigma_s\right)^2 + \left(\tau/\tau_s\right)^2 - 1 = 0,$$

$$\mathbf{D} = \Lambda\,\partial\Phi/\partial\boldsymbol{\sigma}. \quad (5)$$

where functions $\tau_s(\rho)$ and $\sigma_s(\rho)$ are shear and volumetric plastic moduli, respectively; $\sigma = \operatorname{tr}\boldsymbol{\sigma}/3$ is the mean stress, τ is the shear stress intensity, $\tau^2 = \operatorname{tr}\boldsymbol{\sigma}^2/2 - \operatorname{tr}^2\boldsymbol{\sigma}/6$, $\boldsymbol{\sigma}$ is the (macroscopic) Cauchy stress tensor, Λ is a scalar plastic multiplier.

From (5) it follows that (see Appendix A)

$$\frac{\boldsymbol{\sigma}}{\sqrt{2}\tau_s} = \frac{\mathbf{D} + \vartheta\mathbf{I}\operatorname{tr}\mathbf{D}}{\sqrt{\operatorname{tr}\mathbf{D}^2 + \vartheta\operatorname{tr}^2\mathbf{D}}},$$

where $\mathbf{I}$ is the unit tensor, $\vartheta = \left(\sigma_s/\tau_s\right)^2/2 - 1/3$. Hence

$$\frac{\sigma_{rr} - \sigma_{\varphi\varphi}}{\sqrt{2}\tau_s} = \sqrt{1-\lambda}\,\frac{1-L}{\sqrt{L^2 + 2\lambda L + 1}}$$
$$\frac{\sigma_{rr}}{\sqrt{2}\tau_s} = -\frac{1}{\sqrt{1-\lambda}}\frac{L+\lambda}{\sqrt{L^2 + 2\lambda L + 1}}, \quad (6)$$

where $\lambda = \vartheta\left(1+\vartheta\right)^{-1}$.

Substituting (6) into (3), one can obtain nonlinear first-order ODE that determines the function $L(\rho)$. Boundary condition $L(\rho_{out}) = -\lambda(\rho_{out})$ is according to (6) since the surface $r = r_{out}$ is traction-free, i.e. $\sigma_{rr}(r_{out}) = 0$.

With calculated $L(\rho)$, formulas (4) and (6) determine density and pressure in the channel.

3. Green type piecewise-linear yield criterion

Under the plane-strain condition, the following piecewise-linear criterion can be utilized:

$$\Phi = (\sigma_1 - \sigma_3)/(2\tau_s) + |\sigma_1 + \sigma_3|/(2\sigma_s) - 1 = 0. \quad (7)$$

Here σ_1 and σ_3 are the largest and smallest eigenvalues of the stress tensor, respectively. In the problem under consideration it is reasonable to assume that $\sigma_1 = \sigma_{rr}$, $\sigma_3 = \sigma_{\varphi\varphi}$, $\sigma_1 + \sigma_3 < 0$ and according to (7) the following is obtained

$$\sigma_{\varphi\varphi} = \frac{\sigma_s - \tau_s}{\sigma_s + \tau_s}\sigma_{rr} - \frac{2\tau_s\sigma_s}{\sigma_s + \tau_s}. \quad (8)$$

The normality rule associated with (7) leads to the expressions

$$D_{rr} = \Lambda\frac{\sigma_s - \tau_s}{2\sigma_s\tau_s},\; D_{\varphi\varphi} = -\Lambda\frac{\sigma_s + \tau_s}{2\sigma_s\tau_s},$$

$$L(\rho) = \frac{D_{rr}}{D_{\varphi\varphi}} = -1 + \frac{2\tau_s}{\sigma_s + \tau_s}. \quad (9)$$

and according to (4)

$$\ln\frac{r_{out}}{r} = -\frac{1}{2}\left(\ln\frac{\rho_{out}}{\rho} + \int_{\rho}^{\rho_{out}}\frac{\sigma_s}{\tau_s}\frac{dp}{p}\right). \quad (10)$$

Taking into account the equalities (8) and (9), the equilibrium equation (3) takes the form

$$\rho\frac{\partial\sigma_{rr}}{\partial\rho} = \sigma_{rr} + \sigma_s \quad (11)$$

and hence

$$\sigma_{rr} = -\rho\int_{\rho}^{\rho_{out}}\sigma_s(p)\frac{dp}{p^2}. \quad (12)$$

Equations (10) and (12) define the pressure distribution in the channel in a parametric form with the parameter $\rho \in [\rho_{in}, \rho_{out}]$. This solution is valid for $\rho_{in} \geq \rho_*$, where ρ_* can be determined from (12) with $\sigma_{rr}(\rho_*) = -\sigma_s(\rho_*)$. When $\rho_{in} = \rho_*$, the stress state at the inlet of a channel is hydrostatic compression.

4. Results and discussion

The model [29] was utilized to determine the plastic modules:

$$\sigma_s = \frac{2}{\sqrt{3}}\frac{\rho\kappa}{\sqrt{1-\rho}},\; \tau_s = \frac{\sqrt{3}\rho\kappa}{\sqrt{5-2\rho}}.$$

where κ is the shear yield stress of a porosity-free material.

Fig. 2 shows the dimensionless extrusion pressure P/κ, where $P = -\sigma_{rr}|_{r=r_{in}}$, versus area reduction $R = 1 - r_{out}/r_{in}$ calculated according the obtained solutions for different values of initial density.

Fig. 3 shows the density of the material at the inlet of the channel, required to achieve the specified values of relative density at the outlet of the channel.

For comparison, we write down an approximate solution [18] for the Gurson model

$$\rho_{in} = 1 - (1 - \rho_{out})e^{\beta-\alpha},$$

$$P/\kappa = -2\ln(1-R) - \left(2/\sqrt{3}\right)(1-\rho_{in})e^{-\beta}\int_{\alpha}^{\beta}\frac{\xi e^{\xi}}{\sqrt{\xi^2-1}}d\xi,$$

$$\alpha = \cosh\left(\sqrt{3}/2\right),\; \beta = \cosh\left(\sqrt{3}/2 - \sqrt{3}\ln(1-R)\right).$$

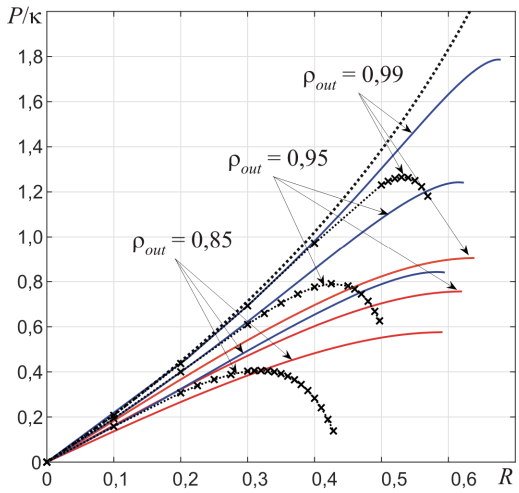

Fig. 2. Extrusion pressure and area reduction required to achieve the specified values of final density: x – Gurson model (solution [18]), blue line – elliptic Green type model (numerical solution), red line – piecewise-linear Green type model (eqs. (10) and (12)), dash line corresponds to $P/\kappa = -2\ln(1-R)$ (incompressible von Mises material)

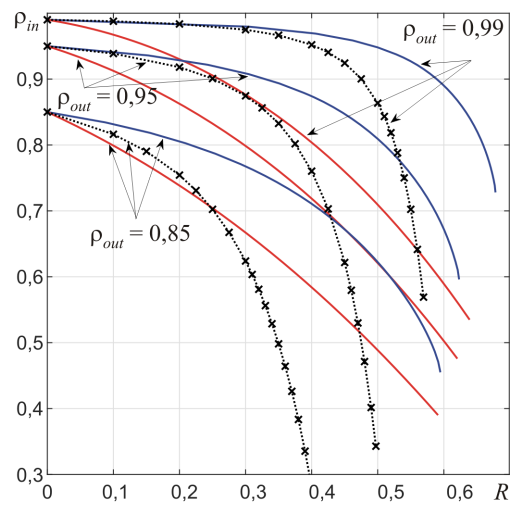

Fig. 3. Initial density and area reduction required to achieve the specified values of final density: x – Gurson model (solution [18]), blue line – elliptic Green type model (numerical solution), red line – piecewise-linear Green type model (eq. (10))

It should be noted regarding the elliptic Green model and Gurson model that extrusion pressure depends nonmonotonically on the area reduction R. With R above a certain value, there is a zone near the channel inlet where the pressure increases in the direction of material motion. This effect is pronounced for the Gurson model and is barely noticeable for the elliptical Green model. In addition, for both models, when area reduction is above a certain value, the compaction begins outside the tapered region.

The extrusion pressure predicted by the piecewise-linear model is lower than what obtained by the elliptic Green model. In turn, the pressure predicted by elliptic Green model is lower than what can be calculated by solution [18], obtained in the frame of Gurson model. At low values of area reduction R, all three models predict approximately the same extrusion pressure. With a small initial porosity of the material, the Gurson model gives results that are close to the elliptic Green model, and with a large initial porosity, to the piecewise-linear Green model.

Appendix A. Stress derivation for Green model

For the yield condition

$$\Phi = \left(\sigma/\sigma_s\right)^2 + \left(\tau/\tau_s\right)^2 - 1 = 0\,;$$

$$\tau^2 = \operatorname{tr}\boldsymbol{\sigma}^2/2 - \operatorname{tr}^2\boldsymbol{\sigma}/6\,, \quad \sigma = \operatorname{tr}\boldsymbol{\sigma}/3$$

the normality rule leads to the following expression for plastic strain rate tensor [30]

$$\mathbf{D} = \Lambda\frac{\partial\Phi}{\partial\boldsymbol{\sigma}} = \frac{\Lambda}{9}\left(\frac{1}{\sigma_s^2} - \frac{3}{2\tau_s^2}\right)\frac{\partial\operatorname{tr}^2\boldsymbol{\sigma}}{\partial\boldsymbol{\sigma}} + \frac{\Lambda}{2\tau_s^2}\frac{\partial\operatorname{tr}\boldsymbol{\sigma}^2}{\partial\boldsymbol{\sigma}} = \\ = \Lambda\left[\left(\frac{2}{3\sigma_s^2} - \frac{1}{\tau_s^2}\right)\frac{\operatorname{tr}\boldsymbol{\sigma}}{3}\mathbf{I} + \frac{\boldsymbol{\sigma}}{\tau_s^2}\right]. \tag{13}$$

Applying the trace operator to both sides of equality (13), we find

$$\operatorname{tr}\mathbf{D} = \Lambda\frac{2\operatorname{tr}\boldsymbol{\sigma}}{3\sigma_s^2}\,. \tag{14}$$

and $\operatorname{tr}\boldsymbol{\sigma} = \left(3\sigma_s^2\operatorname{tr}\mathbf{D}\right)/\left(2\Lambda\right)$. Substituting the last expression in (13), we express the stress tensor as

$$\boldsymbol{\sigma} = -\left(\frac{2\tau_s^2}{3\sigma_s^2} - 1\right)\frac{\sigma_s^2\operatorname{tr}\mathbf{D}}{2\Lambda}\mathbf{I} + \frac{\tau_s^2}{\Lambda}\mathbf{D} \tag{15}$$

and then

$$\boldsymbol{\sigma}^2 = \mathbf{D}^2\frac{\tau_s^4}{\Lambda^2} - \mathbf{D}\frac{2\tau_s^2\operatorname{tr}\mathbf{D}}{\Lambda^2}\left(\frac{\tau_s^2}{3} - \frac{\sigma_s^2}{2}\right) + \mathbf{I}\frac{\operatorname{tr}^2\mathbf{D}}{\Lambda^2}\left(\frac{\tau_s^2}{3} - \frac{\sigma_s^2}{2}\right)^2.$$

Applying the trace operator to both sides of the last equality, we find

$$\operatorname{tr}\boldsymbol{\sigma}^2 = \frac{\tau_s^4}{\Lambda^2}\left[\operatorname{tr}\mathbf{D}^2 + \left(\frac{3\sigma_s^4}{4\tau_s^4} - \frac{1}{3}\right)\operatorname{tr}^2\mathbf{D}\right]$$

and then

$$\tau^2 = \frac{\operatorname{tr}\boldsymbol{\sigma}^2}{2} - \frac{\operatorname{tr}^2\boldsymbol{\sigma}}{6} = \frac{\tau_s^4}{2\Lambda^2}\left(\operatorname{tr}\mathbf{D}^2 - \frac{\operatorname{tr}^2\mathbf{D}}{3}\right).$$

Substituting this expression together with (14) into the yield condition, we obtain the following expression for the plastic multiplier

$$2\left(\frac{\Lambda}{\tau_s}\right)^2 = \operatorname{tr}\mathbf{D}^2 + \left(\frac{1}{2}\frac{\sigma_s^2}{\tau_s^2} - \frac{1}{3}\right)\operatorname{tr}^2\mathbf{D}\,.$$

Substituting this expression into (15), after some algebra, we have

$$\frac{\boldsymbol{\sigma}}{\sqrt{2}\tau_s} = \frac{\mathbf{D} + \vartheta\mathbf{I}\operatorname{tr}\mathbf{D}}{\sqrt{\operatorname{tr}\mathbf{D}^2 + \vartheta\operatorname{tr}^2\mathbf{D}}}\,, \quad \vartheta = \frac{1}{2}\left(\frac{\sigma_s}{\tau_s}\right)^2 - \frac{1}{3}\,.$$

References

1. Breitenbach J. Melt extrusion: From process to drug delivery technology. *Eur. J. Pharm. Biopharm.*, 2002, vol. 54, pp. 107–117. doi: 10.1016/S0939-6411(02)00061-9

2. Singh S., Gamlath S., Wakeling L. Nutritional aspects of food extrusion: A review. *Int. J. Food Sci. Tech.*, 2007, vol. 42, pp. 916–929. doi: 10.1111/j.1365-2621.2006.01309.x

3. Anferov S.D., Skul'skiy O.I., Slavnov E.V. Mathematical modelling of vegetable oil plunger extraction. *PNRPU Mechanics Bulletin*, 2014, no. 1, pp. 31–56. doi: 10.15593/perm.mech/2014.1.31-56

4. Nadai A. Uber die Gleit- und Verzweigungsflachen einiger Gleichgewichtszustande bildsamer Massen und die Nachspannungen bleibend verzerrter Korper. *Z. Phys.*, 1924, vol. 30, pp. 106–138. doi: 10.1007/BF01331828

5. Hill R. Mathematical theory of plasticity. 1950. Clarendon Press, Oxford.

6. Sokolovsky V.V. Planar and axisymmetric equilibrium of the plastic mass between rigid walls. *J. Appl. Math. Mech.*, 1950, vol. 14, pp. 75–92.

7. Durban D., Budiansky B. Plane-strain radial flow of plastic materials. *J. Mech. Phys. Solids*, 1978, vol. 26, no. 5, pp. 303–324. doi: 10.1016/0022-5096(78)90002-9

8. Haddow J.B., Danyluk H.T. The flow of an incompressible elastic-perfectly plastic solid. *Acta Mech.*, 1968, vol. 5, pp. 14–21. doi: 10.1007/BF01624440

9. Avitzur B., Fueyo J., Thompson J. Analysis of plastic flow through inclined planes in plane strain. *J. Eng. Ind. – T. ASME*, 1967, vol. 89, no. 2, pp. 361–375. doi: 10.1115/1.3610053

10. Avitzur B., Choi J.C. Analysis of central bursting defects in plane strain drawing and extrusion, *J. Eng. Ind. – T. ASME*, 1986, vol. 108, no. 4, pp. 317–321. doi: 10.1115/1.3187082

11. Alexandrov S., Mustafa Y., Hwang Y.-M., Lyamina E. An accurate upper bound solution for plane strain extrusion through a wedge-shaped die, *The Scientific World Journal*, 2014, vol. 2014, 189070. doi: 10.1155/2014/189070

12. Alexandrov S., Kuo C.-Y., Jeng Y.-R. An accurate numerical solution for the singular velocity field near the maximum friction surface in plane strain extrusion. *Int. J.*

Solids Struct., 2018, vol. 150, pp. 107-116. doi: 10.1016/j.ijsolstr.2018.06.006

13. Thore P., Pastor F., Pastor J., Kondo D. Closed-form solutions for the hollow sphere model with Coulomb and Drucker – Prager materials under isotropic loadings. *CR Mecanique*, 2009, vol. 337, pp. 260–267. doi: 10.1016/j.crme.2009.06.030
14. Monchiet V., Kondo D. Exact solution of a plastic hollow sphere with a Mises – Schleicher matrix. *Int. J. Eng. Sci.*, 2012, vol. 51, pp. 168–178. doi: 10.1016/j.ijengsci.2011.10.007
15. Dos Santos T., Vadillo G. A closed-form yield criterion for porous materials with Mises – Schleicher – Burzynski matrix containing cylindrical voids. *Acta Mech.*, 2021, vol. 232, pp. 1285–1306. doi: 10.1007/s00707-020-02925-y
16. Green R.J. A plasticity theory for porous solids. *Int. J. Mech. Sci.*, 1972, vol. 14, pp. 215–224. doi: 10.1016/0020-7403(72)90063-X
17. Gurson A.L. Continuum theory of ductile rupture by void nucleation and growth: Part 1 – yield criteria and flow rules for porous ductile media. *J. Eng. Mater. – T. ASME*, 1977, vol. 99, pp. 2–15. doi: 10.1115/1.3443401
18. Durban D., Mear M.E. Asymptotic solution for extrusion of sintered powder metals. J. *Appl. Mech. – T. ASME*, 1991, vol. 58, pp. 582–584. doi: 10.1115/1.2897226
19. Tirosh T., Iddan D. Forming analysis of porous materials. *Int. J. Mech. Sci.*, 1989, vol. 31, pp. 949–965. doi: 10.1016/0020-7403(89)90035-0
20. Govindarajan R.M., Aravas N. Asymptotic analysis of extrusion of porous metals. *Int. J. Mech. Sci.*, 1991, vol. 33, pp. 505–527. doi: 10.1016/0020-7403(91)90014-T
21. Saleh Ch.A.R., Ragab A.R., Samy S.N. Prediction of void growth in drawing and extrusion of voided metals. *Mech. Mater.*, 2005, vol. 37, no. 9, pp. 915–924. doi: 10.1016/j.mechmat.2004.09.004
22. Kailasam M., Aravas N., Ponte Castaneda P. Porous metals with developing anisotropy: Constitutive models, computational issues and applications to deformation processing. *CMES – Computer Modeling in Engineering & Sciences*, 2000, vol. 1, no. 2, pp. 105–118. doi: 10.3970/cmes.2000.001.265
23. Aleksandrov S.E., Druyanov B.A. Investigating the process of the steady extrusion of a compacted material. *J. Appl. Mech. Tech. Phy.*, 1991, vol. 31, no. 4, pp. 645–649. doi: 10.1007/BF00851344
24. Alexandrov S., Chesnikova O., Pirumov A. An approximate solution for axisymmetric extrusion of porous material. *J. Technol. Plasticity*, 2007, vol. 32, pp. 13–27.
25. Sevastyanov G.M., Sevastyanov A.M. Approximate analysis of extrusion process for Green type porous material. *Mech. Solids*, 2021, vol. 56, no. 7, pp. 1363–1372. doi: 10.3103/S0025654421070220
26. Sevastyanov G.M. Filtration in fluid-saturated poro-plastic materials during lateral extrusion. *PNRPU Mechanics Bulletin*, 2019, vol. 2, pp. 163–171. doi: 10.15593/perm.mech/2019.2.13
27. Sevastyanov G.M., Sevastyanov A.M. Filtration and heat processes in lateral extrusion of plasticallycompressible materials. *J. Phys.: Conf. Ser.*, 2019, vol. 1203, 012022. doi: 10.1088/1742-6596/1203/1/012022
28. Mear M.E., Durban D. Radial flow of sintered powder metals. *Int. J. Mech. Sci.*, 1989, vol. 31, pp. 37–49. doi: 10.1016/0020-7403(89)90117-3
29. Ponte Castaneda P. The effective mechanical properties of nonlinear isotropic composites. *J. Mech. Phys. Solids*, 1991, vol. 39, pp. 45–71. doi: 10.1016/0022-5096(91)90030-R
30. Itskov M. Tensor algebra and tensor analysis for engineers with applications to continuum mechanics. 2015. *Springer International Publishing, Switzerland*.

Финансирование. Исследование выполнено при финансовой поддержке РФФИ в рамках научного проекта № 20-01-00147.
Конфликт интересов. Автор заявляет об отсутствии конфликта интересов.

Financing. This work was supported by RFBR (grant number 20-01-00147).
Conflict of interest. The authors declare no conflict of interest.